# Hyperforin—a key constituent of St. John's wort specifically activates TRPC6 channels

Kristina Leuner,\* Victor Kazanski,<sup>†</sup> Margarethe Müller,\* Kirill Essin,<sup>‡</sup> Bettina Henke,\* Maik Gollasch,<sup>‡</sup> Christian Harteneck,<sup>†</sup> and Walter E. Müller\*

\*Pharmakologisches Institut für Naturwissenschaftler, Biocenter Niederursel, Frankfurt, Germany; 
†Molekulare Pharmakologie und Zellbiologie, Charité—Universitätsmedizin Berlin, Berlin, Germany; 
and †Charité University Medicine, Section Nephrology/Intensive Care, Campus Virchow, and Franz 
Volhard Clinic at the Max Delbrück Center Berlin-Buch, Berlin, Germany

ABSTRACT Hyperforin, a bicyclic polyprenylated acylphloroglucinol derivative, is the main active principle of St. John's wort extract responsible for its antidepressive profile. Hyperforin inhibits the neuronal serotonin and norepinephrine uptake comparable to synthetic antidepressants. In contrast to synthetic antidepressants directly blocking neuronal amine uptake, hyperforin increases synaptic serotonin and norepinephrine concentrations by an indirect and yet unknown mechanism. Our attempts to identify the molecular target of hyperforin resulted in the identification of TRPC6. Hyperforin induced sodium and calcium entry as well as currents in TRPC6-expressing cells. Sodium currents and the subsequent breakdown of the membrane sodium gradients may be the rationale for the inhibition of neuronal amine uptake. The hyperforin-induced cation entry was highly specific and related to TRPC6 and was suppressed in cells expressing a dominant negative mutant of TRPC6, whereas phylogenetically related channels, i.e., TRPC3 remained unaffected. Furthermore, hyperforin induces neuronal axonal sprouting like nerve growth factor in a TRPC6dependent manner. These findings support the role of TRPC channels in neurite extension and identify hyperforin as the first selective pharmacological tool to study TRPC6 function. Hyperforin integrates inhibition of neurotransmitter uptake and neurotrophic property by specific activation of TRPC6 and represents an interesting lead-structure for a new class of antidepressants.—Leuner, K., Kazanski, V., Müller, M., Essin, K., Henke, B., Gollasch, M., Harteneck, C., Müller, W. E. Hyperforin—a key constituent of St. John's wort specifically activates TRPC6 channels. FASEB J. 21, 4101-4111 (2007)

Key Words: calcium · neurite outgrowth

HYPERFORIN, A PHLOROGLUCINOL DERIVATE (Fig. 1A), is the main active ingredient of St. John's wort extract (1), which is widely used as the herbal alternative to treat depression. In 2002, 12% of U.S. adults were reported to have used St. John's wort extract within the last 12 months (2). Several recent clinical trials (3–5)

and Cochrane meta-analysis confirm the clinical efficacy and good tolerability of St. John's wort for mild to moderate depression (6). Like most synthetic antidepressants, hyperforin interferes with the neuronal uptake of serotonin, dopamine, and norepinephrine (1, 7–9). Whereas synthetic antidepressants are competitive inhibitors of the respective transporter proteins, hyperforin reduces monoamine uptake by elevating the intracellular sodium concentration ([Na<sup>+</sup>]<sub>i</sub>) and thereby decreasing the sodium gradient as the driving force of these neurotransmitter transporters (7, 8). We have previously shown concentration-dependent elevations of  $[\mathrm{Na^+}]_i$  and  $[\mathrm{Ca^{2+}}]_i$  by hyperforin with  $\mathrm{EC}_{50}$  values for  $\mathrm{Na^+}$  of 0.72  $\mu\mathrm{M}$  and for  $\mathrm{Ca^{2+}}$  of 1.16  $\mu\mathrm{M}$ . Hyperforin-induced Ca<sup>2+</sup> and Na<sup>+</sup> influx was not mediated by voltage-dependent sodium or calcium channels (9). We hypothesized that hyperforin activates a nonselective cation channel, the identity of which needs to be clarified.

One group of nonselective cation channels is transient receptor potential (TRP) channels. TRP channels are a superfamily of functionally versatile cation channels that are present in most mammalian cell types. According to their primary structure, mammalian TRP proteins are classified into at least six subgroups, the TRPC, TRPV, TRPM, TRPP, TRPML, and TRPA subfamilies (10, 11). Some typical functional features can be assigned particularly to the three main subfamilies, the classic or canonical TRPs (TRPC), the vanilloid receptor-related TRPs (TRPV), and the melastatinrelated TRPs (TRPM): the seven TRPC members are characterized by their activation due to stimulation of G-protein-coupled receptors and phospholipase C (PLC). Four of the six TRPV channels are activated by increases in temperature and are probably involved in heat and pain sensation in human body. TRPM channels (eight members) show an activation by different stimuli and possess a quite variable permeability for divalent cations (12-14). TRPC channels are widely

<sup>&</sup>lt;sup>1</sup> Correspondence: Pharmakologisches Institut für Naturwissenschaftler, Max-von-Laue-Strasse 9, 60438 Frankfurt, Germany. E-mail: pharmacolnat@em.uni-frankfurt.de doi: 10.1096/fj.07-8110com

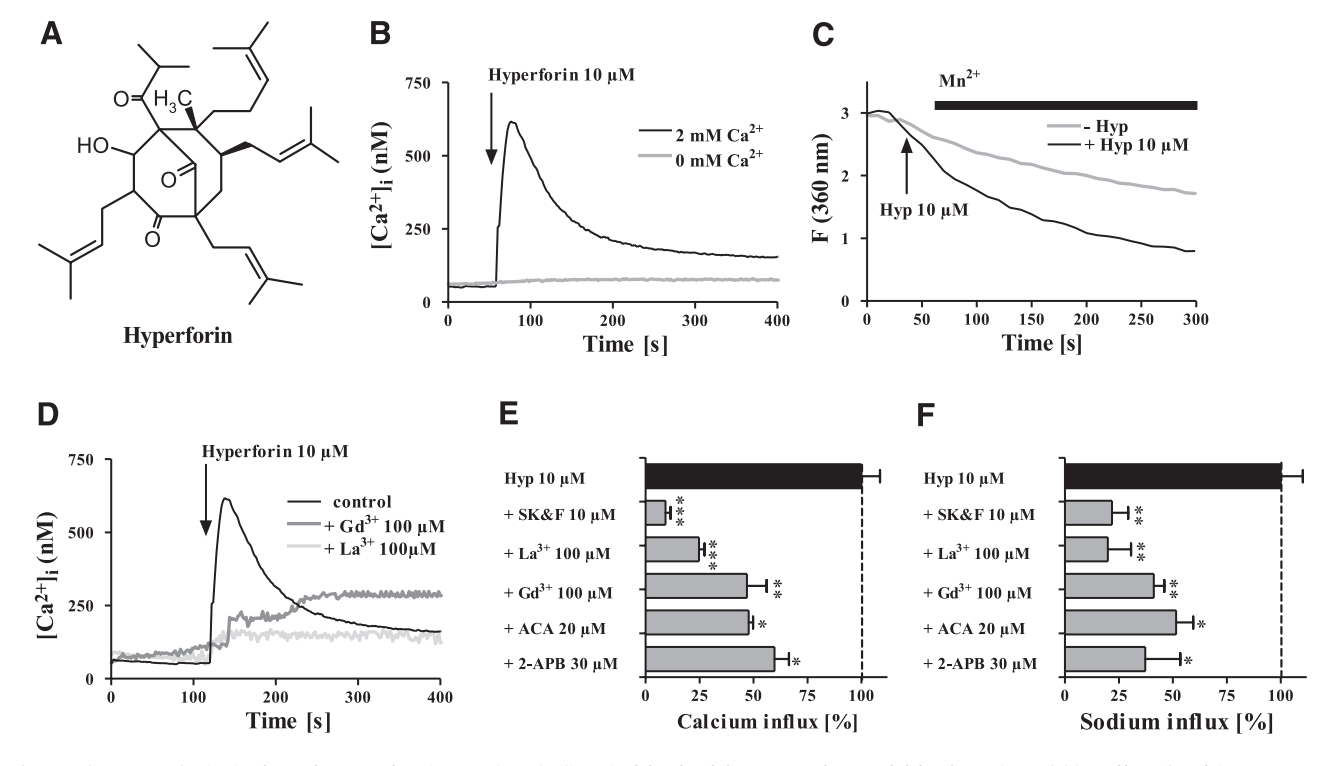


Figure 1. Hyperforin-induced nonselective cation influx is blocked by TRP channel blockers in PC12 cells. *A*) This structure represents the chemical structure of the phloroglucinol derivative hyperforin. *B*) Hyperforin-induced changes in  $[Ca^{2+}]_i$  were characterized in fura-2-loaded PC12 cells in cell suspension experiments as described in Materials and Methods. Representative time traces show dependence of hyperforin-induced elevation of  $[Ca^{2+}]_i$  from the presence of extracellular calcium (2 mM), arguing for the activation of an entry mechanism by hyperforin (10 μM; n=6). *C*) Hyperforin-mediated cation influx was characterized by experiments using  $Mn^{2+}$  quench of fura-2 fluorescence. Fluorescence of fura-2 at isosbestic wavelength of fluorophore at 360 nm was determined in fura-2-loaded PC12 cells.  $Mn^{2+}$  (100 μM) was added 20 s after starting to record. Hyperforin (10 μM) was added subsequently. Traces represent averaged traces from 6 independent experiments. Mean time traces of hyperforin (10 μM) compared to control cells show that hyperforin is able to induce  $Mn^{2+}$  influx in PC12 cells. *D*, *F*) To identify the molecular structure of the hyperforin-activated entry mechanism, we tested the effects of different TRP channel blockers on hyperforin-induced  $Na^{+}$  and  $Ca^{2+}$  influx. *D*) Single time traces of a representative experiment show effect of hyperforin (10 μM) in the presence and absence of  $La^{3+}$  (100 μM) or  $Gd^{3+}$  (100 μM).  $La^{3+}$  and  $Gd^{3+}$  were added 2 min before start of measurement. Hyperforin (10 μM) was added 120 s after start of experiment. *E*)  $Na^{+}$  influx was measured with the fluorescence dye SBFI. Summary of changes in  $[Ca^{2+}]_i$  and  $[Na^{+}]_i$  in percentage induced by hyperforin in the absence and presence of SK&F 96365 (10 μM, n=6),  $LA^{3+}$  (100 μM, n=6),  $Cd^{3+}$  (10

expressed in the brain (15, 16). Increasing evidence suggests that TRPC channels play an important role for growth cone guidance and neurite extension in the brain (17–19). TRPC1, TRPC3, and TRPC6 are activated by the brain-derived neurotrophic factor (BDNF) and affect growth cone morphology and axonal growth in primary neuronal cultures (17, 18).

Here, we show that hyperforin-induced calcium entry in PC12 is specifically mediated by TRPC6 channels. Testing several TRPC channels revealed that hyperforin selectively stimulates TRPC6, whereas other members of the TRPC group remain unaffected. Electrophysiological characterization of hyperforin-induced currents showed characteristics comparable with earlier data published for TRPC6 activated by receptor stimulation. In addition to the rapid hyperforin-induced responses affecting intracellular calcium and sodium concentrations, long-term incubation of PC12 cells, endogenously expressing TRPC6, results in enhanced neurite

outgrowth. Hyperforin-treated cells showed neurite outgrowth comparable to nerve growth factor (NGF)-treated cells. The dependence of hyperforin-induced calcium entry and induction of axonal outgrowth on functional expressed TRPC6 argue that the hyperforin-induced antidepressive profile results from a specific activation of neuronal expressed TRPC6 channels.

### MATERIALS AND METHODS

### Sources and preparation of reagents

Hyperforin was a kind gift of Dr. Willmar Schwabe, Karlsruhe (Germany). 1-oleoyl-2-acetyl-sn-glycerol (OAG; Sigma-Aldrich, Taufkirchen, Germany) was used from 100 mM stock solution in dimethyl sulfoxide. Flufenamic acid (FFA; Sigma-Aldrich) and N-(p-amylcinnamoyl) anthranilic acid (ACA;

Calbiochem, San Diego, CA, USA) were used from 50 mM stock solution in dimethyl sulfoxide.

2-Aminophenoxyborate (2-APB) was from Tocris (Avonmouth, UK). NGF (Sigma-Aldrich) was dissolved in distilled water and prepared in 50  $\mu g/ml$  stock solution. GdCl $_3$ , LaCl $_3$  (Sigma-Aldrich) were dissolved in  $H_2O$  before experiments. Other chemicals were dissolved in DMSO in  $1000\times$  stock solution, and diluted before use. For pharmacological treatments, chemicals were present throughout the experiment

## Cell culture and transfection of HEK293 cells and PC12 cells

HEK293 cells were cultured in Dulbecco's modified Eagle's medium (DMEM; Invitrogen, Groningen, The Netherlands) with 10% heat-inactivated fetal calf serum (Sigma-Aldrich), 50 U/ml penicillin (Sigma-Aldrich), and 50  $\mu g/ml$  streptomycin (Sigma-Aldrich) at 37°C under a 5% CO $_2$  humidified atmosphere at 37°C. Cells were plated in 85 mm dishes onto glass cover slips and transiently transfected 24 h later by addition of a transfection cocktail containing 0.5 to 1  $\mu g$  of DNA and 1 to 2  $\mu l$  of FuGENE 6 transfection reagent (Roche Diagnostics, Indianapolis, IN, USA) in 97  $\mu l$  of Opti-MEM medium (Invitrogen). The cDNA constructs have been kindly provided by Dr. Michael Schaefer (20). Fluorescence measurements and electrophysiological studies were carried out 1 to 2 days after transfection.

PC12 cells were cultured in DMEM supplemented with 10% heat-inactivated fetal calf serum and 5% heat-inactivated horse serum, 50 U/ml penicillin, and 50  $\mu$ g/ml streptomycin at 37°C in a humidified incubator containing 5% CO<sub>2</sub>. Before Ca<sup>2+</sup> imaging, cells were plated in 85 mm dishes onto glass cover slips. Transient transfection of PC12 cells was conducted using FuGENE 6 transfection reagent (Roche Diagnostics). Cells were plated in 85 mm dishes onto glass cover slips and transiently transfected by addition of a transfection cocktail containing 0.5 to 1  $\mu$ g of DNA and 2  $\mu$ l of FuGENE 6 transfection reagent (Roche Diagnostics) in 97  $\mu$ l of Opti-MEM medium (Invitrogen). Fluorescence measurements were conducted 2 days after transfection. Neurite outgrowth assays were conducted 3 to 5 days after transfection.

For TRPC6 knock-down studies with siRNA, PC12 cells (2 Mio.) were suspended in DMEM containing 2% serum and were mixed with 200 nM TRPC6 siRNA (RNAi 1: UUUAAAUGGAAAUCUUCUGAGCUCC; RNAi 2: AAAC-CACCGCGAUUGCAUAA-AGACA; RNAi 3: UUCAGCUG-CAUCCAGAAAGCGUUCC) or a control sequence with low or medium GC content, each with its complementary sequence. We used Stealth (Invitrogen) siRNA sequences developed to eliminate nonspecific stress responses of the PKC/interferon pathway induced by siRNA. PC12 cells together with siRNA were electroporated using the Gene Pulser II electroporation system (Bio-Rad) at 220 V, 550 μF. After 10 min recovery period on ice, cells were incubated in the same medium for 48 h on coverslips coated with poly-L-lysine before fura-2 imaging was undertaken. Neurite outgrowth assays were conducted 3-5 days after transfection.

#### Western blotting

PC12 cells were harvested by centrifugation (800 g, 5 min, room temperature). Cells were resuspended in lysis buffer (50 mM Tris/HCl, 2 mM DTT, 0.2  $\mu$ M benzamidine, and 1 mM EDTA, pH 8.0) and homogenized by shearing through 26 gauge needles. After removal of nuclei (800 g, 2 min, 4°C), supernatants were mixed with gel loading buffer (62.5 mM

Tris/HCl, 10% glycerol, 5% mercaptoethanol, and 2% SDS, 0.02% bromphenol blue, pH 6.8). After electrophoresis, the proteins were transferred on nitrocellulose membrane. One half of the membrane was incubated with polyclonal rabbit anti-TRPC6 antibody (Chemicon) 1:300 overnight. The second part was incubated with the antibody (20  $\mu g$ ) in the presence of antigenic peptide (20  $\mu g$ ). The antibodies were visualized by incubation with horseradish-antibody conjugate. For RNAi experiments, cells were incubated with polyclonal rabbit anti-TRPC6 antibody or with polyclonal mouse anti-GAPDH (Invitrogen) overnight. Again, the antibodies were visualized by incubation with horseradish-antibody conjugate.

### Fluorescence measurements

[Ca<sup>2+</sup>]<sub>i</sub> measurements in single cells were carried out using the fluorescence indicator fura-2-AM in combination with a monochromator-based imaging system (T.I.L.L. Photonics, Martinsried, Germany, or Attofluor Ratio Vision system) attached to an inverted microscope (Axiovert 100, Carl Zeiss, Oberkochen, Germany). HEK293 cells and PC12 cells were loaded with 4 µM fura-2-AM (Invitrogen) and 0.01% Pluronic F-127 (Invitrogen) for 45 min at room temperature in a standard solution composed of 138 mM NaCl, 6 mM KCl, 1 mM MgCl<sub>2</sub>, 2 mM CaCl<sub>2</sub>, 5.5 mM glucose, and 10 mM HEPES (adjusted to pH 7.4 with NaOH). Cover slips were then washed in this buffer for 20 min and mounted in a perfusion chamber on the microscope stage. For [Ca<sup>2+</sup>]<sub>i</sub> measurements, fluorescence was excited at 340 and 380 nm. After correction for background fluorescence, the fluorescence ratio  $F_{340}/F_{380}$  was calculated. Fluorescence quenching by Mn<sup>2+</sup> entry was studied using the fura-2 isosbestic excitation wavelength at 360 nm, and the emitted light was monitored using the same filter system as for [Ca<sup>2+</sup>]<sub>i</sub> measurements. In all experiments, transfected cells (5-10 cells) of the whole field of vision were identified by their YFP fluorescence at an excitation wavelength of 480 nm.

Na<sup>+</sup> and Ca<sup>2+</sup> measurement in cell suspension was conducted using quartz cuvettes and a SLM-Aminco luminescence spectrometer (Luminescence Spectrometer Series 2, SLM-Aminco; Spectronic Instruments). For loading with the Na<sup>+</sup> fluorescence dye SBFI-AM (Invitrogen), "3K<sup>+</sup>-Ca<sup>2+</sup> without Na<sup>+</sup> Medium" (3 mM KCl, 2 mM MgCl, 5 mM Tris, and 10 mM glucose; the sodium replaced by an equimolar amount of sucrose; pH adjusted with HCl to 7.4) was used. Before loading, PC12 cells were plated at a density of  $1 \times 10^6$  cells/ plate and loaded with 10 µM SBFI-AM for 60 min. After the fluorescence dye was washed out, aliquots of PC12 cells (1 Mio.) were resuspended in Na<sup>+</sup>-containing medium. For  $Ca^{2+}$  imaging, PC12 cells were plated at a density of  $1 \times 10^6$ cells/plate and loaded with 4 µM fura-2-AM and 0.01% Pluronic F-127 for 45 min at room temperature in a standard solution HBSS composed of 138 mM NaCl, 6 mM KCl, 1 mM MgCl<sub>2</sub>, 2 mM CaCl<sub>2</sub>, 5.5 mM glucose, and 10 mM HEPES (adjusted to pH 7.4 with NaOH). After the fluorescence dye was washed out, aliquots of PC12 cells (1 Mio.) were resuspended in HBSS.

### Patch clamp measurements

Membrane currents were recorded using the whole-cell, inside-out, and outside-out configurations of the patch-clamp technique at room temperature (22–24°C). Pipettes were made from borosilicate glass capillary tubes. The pipettes' resistance varied between 2 and 5 M $\Omega$  in whole cell recordings and between 7 and 9 M $\Omega$  in single channel recordings. Whole cell currents were elicited by voltage ramps from –100

to  $\pm 100$  mV (400 ms duration) applied every 10 s from a holding potential of 0 mV. Currents through the pipette were recorded by an Axopatch 200B amplifier (Axon Instruments), filtered at 5 or 10 kHz (Bessel filter), and analyzed using pCLAMP software (version 9.2; Axon Instruments). Pipettes for whole cell recordings were filled with a solution composed of 130 mM CsCH<sub>3</sub>O<sub>3</sub>S, 10 mM CsCl, 2 mM MgCl<sub>2</sub>, and 10 mM HEPES (pH 7.2 with CsOH). The standard bath solution contained 135 mM NaCl, 5 mM KCl, 2 mM CaCl<sub>2</sub>, 1 mM MgCl<sub>2</sub>, 10 mM glucose, and 10 mM HEPES (pH 7.4 with NaOH).

Single-channel currents were continuously measured at different pipette potentials  $(V_p)$ . The corresponding membrane potentials for inside-out patches were calculated by Equation 1,

$$V_m = -V_p + V_L \tag{1}$$

where  $V_m$  is the membrane potential, and  $V_L$  is the junction potential. Pipettes were either filled with 130 mM CsCH<sub>3</sub>O<sub>3</sub>S, 10 mM CsCl, 2 mM MgCl<sub>2</sub>, and 10 mM HEPES (pH 7.4 with CsOH) for inside-out recordings or with 130 mM NaCl, 2 mM CaCl<sub>2</sub>, 1 mM MgCl<sub>2</sub>, and 10 mM HEPES (pH 7.4 with NaOH) for cell attached recordings. In outside-out recordings the bath solution contained 135 mM NaCl, 5 mM CsCl<sub>2</sub>, 2 mM CaCl<sub>2</sub>, 1 mM MgCl<sub>2</sub>, 10 mM glucose, and 10 mM HEPES (pH 7.4 with NaOH); the pipette solution contained 145 mM CsCl, 3 mM MgATP, 0.2 mM EGTA, 0.13 mM CaCl<sub>2</sub>, 20 mM glucose, and 10 mM HEPES (pH 7.3 with CsOH), corresponding to a free [Ca<sup>2+</sup>] of ~100 nM. Single-channel amplitudes at different  $V_m$  values were calculated from current traces of 2–4 s obtained in inside-out and 50 s in outside-out experiments using amplitude histograms fitted to Gaussian functions.

### Neurite outgrowth of PC12 cells

Cells were plated at a density of  $10^4$  cells/plate (85 mm, polylysin coated) in 15% serum containing medium overnight. The next day, medium was changed to a medium containing 2% serum and NGF (50 ng/ml), hyperforin, or hyperforin supplemented with La³+ or Gd³+. The neurite length was examined 3 or 5 days after different treatment regimes. After 3–5 days PC12 cells were fixed with paraformaldehyde solution (4%) and stained with Mayer's hematoxylin & eosin solutions. 10 cells from each stain (n=1) were arbitrarily investigated and neurite length was detected by using Nikon NIS Elements AR 2.1 software.

### **RESULTS**

# TRP channel blockers inhibit hyperforin induced calcium and sodium influx

To identify the molecular target of hyperforin, we used  $Ca^{2+}$  imaging approaches. Hyperforin (10  $\mu$ M) reproducibly induced rapid and transient elevation of intracellular calcium concentration ( $[Ca^{2+}]_i$ ) in 2 mM  $Ca^{2+}$ -containing medium (Fig. 1*B*). Application of  $Ca^{2+}$ -free medium (see Fig. 1*B*) or EGTA-containing medium (data not shown) abolished the increase in  $[Ca^{2+}]_i$ , indicating that hyperforin-induced  $[Ca^{2+}]_i$  elevation is mainly mediated by an influx mechanism across the plasma membrane. The  $[Ca^{2+}]_i$  increase was

not attenuated by thapsigargin  $(1 \mu M)$ , which depletes intracellular calcium stores (data not shown).

For further characterization of the hyperforin-induced calcium entry mechanism, we tested whether hyperforin is able to induce  $Mn^{2+}$  influx (100  $\mu$ M; refs. 21, 22) in PC12 cells by measuring the quench of fura-2 fluorescence. As shown in Fig. 1C, hyperforin enhanced manganese entry additionally supporting the hypothesis that hyperforin acts via a nonselective cation channel. Next, we tested gadolinium and lanthanum ions as nonspecific inorganic blockers of a great variety of cation channels. Hyperforin-induced calcium as well as sodium entry was dramatically reduced in the presence of 100 µM gadolinium and lanthanum ions (Fig. 1D-F). To further characterize and narrow down the identity of the putative cation channel, we tested the effects of several pharmacological tools described to interfere with nonselective cation channels (Fig. 1E, F), i.e., SK&F 96365, 2-APB, and ACA. As shown in Fig. 1E, F, hyperforin-induced Ca<sup>2+</sup> and Na<sup>+</sup> influx was reduced by SK&F 96365 (10 μM), 2-APB, and ACA (30 μM). As the profile of the compounds strongly argued for the involvement of TRP channels in the hyperforin-induced activation of PC12 cells, we also tested ruthenium red (RR; 10 µM), which blocks TRPV, TRPM6, TRPM8, and TRPA1 channels. RR had no effect on hyperforin-induced calcium entry (data not shown) and thereby allowed us to narrow down the variety of putative candidates mainly to TRPC channels. TRPC are nonselective, weakly voltage-dependent channels activated by G-Protein coupled or tyrosine kinase receptors via phosphatidyl inositol signal transduction pathways (23).

# Hyperforin-induced calcium entry in PC12 cells is mediated by TRPC6 channels

To identify the protein mediating the hyperforin-induced calcium entry in PC12 cells, we performed RT-PCR analyses of PC12 cells showing the expression of TRPC1 and TRPC6 in PC12 cells (data not shown). To clarify the presence of the TRPC6 proteins, we performed Western blot analyses. Using a commercially available anti-TRPC6 antibody, we were able to detect a protein with the appropriate molecular mass in membrane extracts of PC12 cells (**Fig. 2***A*, lane A). The specificity of the detection reaction was verified in parallel experiments performed in the presence of the peptide used for immunization (Fig. 2*A*, lane B).

The data so far strongly argued for the involvement of TRPC6 in hyperforin-induced calcium entry. However, the final proof was missing. Therefore, we tested strategies selectively inactivating TRPC6. From the methods available and described, we first chose the knock-down of TRPC6 via transfection of PC12 cells with siRNAs directed against TRPC6 (Fig. 2*B*, *C*). For optimization of experimental condition, we chose Western blot analyses. We analyzed membrane fractions of PC12 cells electroporated with control as well as three different anti-TRPC6 siRNAs abbreviated with RNAi

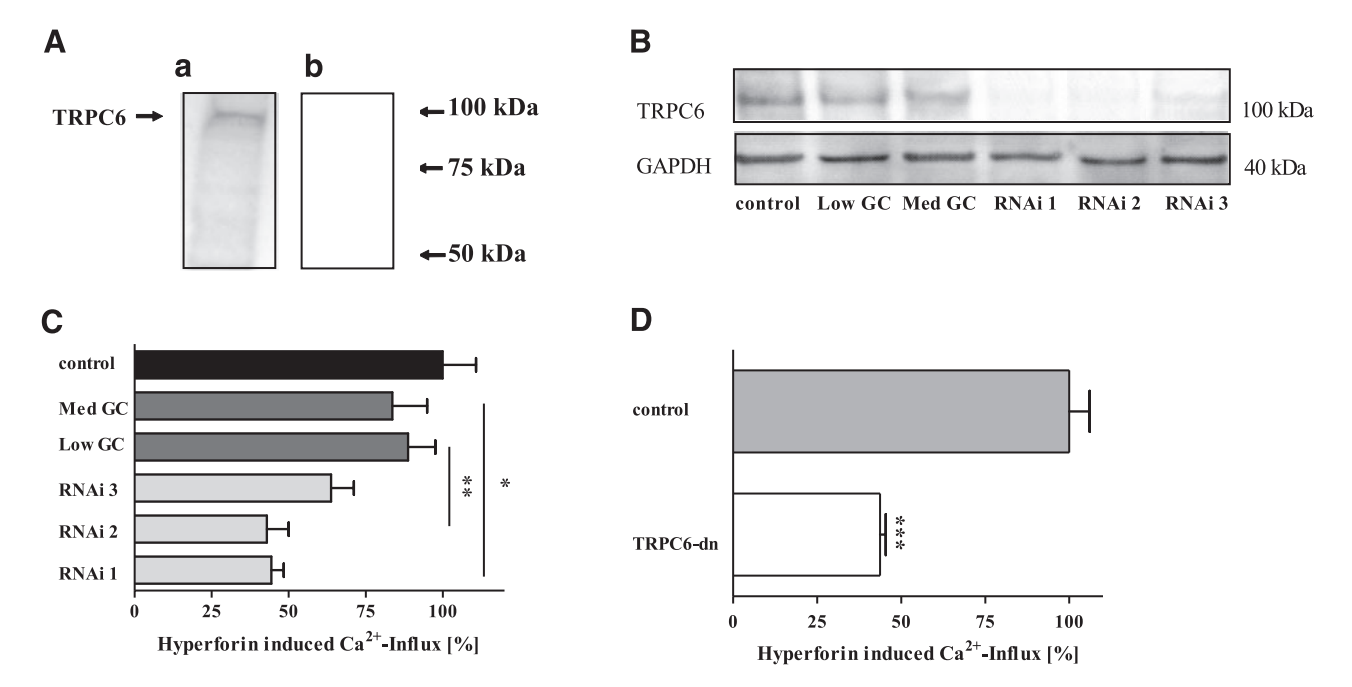


Figure 2. TRPC6 channel expression in PC12 cells A) Membrane fractions of PC12 cells were isolated and analyzed by Western blot analysis. Staining with an anti-TRPC6 antibody resulted in a single band with a molecular mass of around 97 kDa (a). Specificity of reaction was controlled by incubating anti-TRPC6 antibody in the presence of peptide used for immunization (b). B) PC12 cells were electroporated with anti-TRPC6 RNAis (RNAi 1, 2, and 3) and control RNAis with medium GC content (med GC) or low GC content (low GC). In addition, cells only electroporated were used as additional control. Membrane fractions of electroporated PC12 cells were extracted and analyzed by Western blot using anti-GAPDH and anti-TRPC6 antibodies. Comparability was achieved by GAPDH-normalizing of protein load. Shown is 1 representative experiment out of 4 electroporation-experiments. C) PC12 cells were electroporated with RNAi 1, 2, and 3 or in the presence or absence of RNAi of low or medium GC content as control. After an incubation period of 48 h, cells were loaded with fura-2 and were stimulated with hyperforin (n=3, 10–20 cells/independent experiment; \*P<0.05 med GC vs. RNAi 1, \*P<0.01 low GC vs. RNAi 2, unpaired t test). D) fura-2-loaded, TRPC6-DN-YFP expressing PC12 cells were stimulated with hyperforin and compared with untransfected cells (n=6, 5–10 cells/independent experiment; \*v=0.001, unpaired v=1 test).

1–3 (see Fig. 2B). Due to differences in GC content of the anti-TRPC6 siRNAs, we used a random RNAi with medium GC content to control RNAi 1 and 3 and RNAi with low GC content to control RNAi 2. In preparations of PC12 cells transfected with anti-TRPC6 RNAi 1 and 2, the signals were dramatically reduced, whereas in PC12 cells transfected with anti-TRPC6 RNAi 3, TRPC6 protein was still detectable. In control siRNA-electroporated PC12 cells, TRPC6 protein was still detectable; the anti-TRPC6 antibody detected a protein of the appropriate molecular mass. The reduced signal intensities in the Western blot analyses provide evidence for the effectiveness of the anti-TRPC6 siRNAs in knocking down the translation of TRPC6 protein and also argue for the specificity of the selected anti-TRPC6 antibody. In further experiments, we tested whether hyperforininduced calcium entry can be detected in PC12 cells electroporated with anti TRPC6 RNAi 1-3 (see Fig. 2C). The presence of hyperforin-induced calcium entry in control siRNA-electroporated PC12 showed that the hyperforin-induced calcium entry was not affected by the electroporation procedure. In control siRNA-electroporated PC12 cells, hyperforin-induced calcium entry was similar to untreated PC12 cells. By contrast, the increase in calcium was significantly diminished in PC12 cells electroporated in the presence of anti-TRPC6 RNAi 1 and 2 (see Fig. 2C). In anti-TRPC6 RNAi

3 electroporated cells, hpyerforin-induced calcium entry was lessened, but the reduction was too small to be classified as a significant reduction of calcium influx, which mirrors the data of the Western blot analysis. The significantly reduced calcium entry in RNAi 1 and 2-electroporated cells argued for a hyperforin-induced TRPC6-mediated entry mechanism.

As a second method to test the hypothesis of the activation of TRPC6 by hyperforin, we studied hyperforin-induced calcium entry in PC12 cells expressing a dominant negative TRPC6 mutant (Fig. 2D). Several experimental approaches demonstrated that TRPC channel pores, like the pores of cyclic nucleotide-gated cation channels, are formed by homo- or heterotetrameric protein complexes (24, 25). The multimerization of TRPC channels proteins is still not completely understood; nevertheless, it has been shown in several studies that the function of a multimeric channel complex depends on the integrity of the proteins involved. On the other hand, this knowledge enables approaches to specifically inactivate TRP channels by the expression of TRPC proteins mutated in the poreforming region. The specificity of these approaches results from data that all TRPC channels assemble into homo- and heteromers within the confines of TRPC channel subfamilies, e.g., TRPC3/6/7 and TRPC4/5 (24). In several studies, it has been shown that the

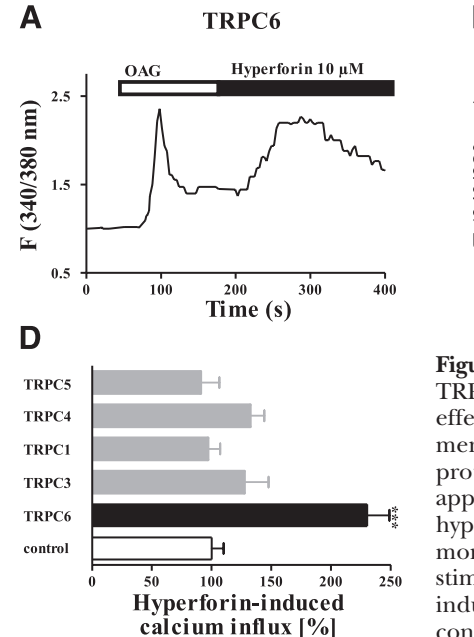
exchange of a highly conserved protein motif within the putative pore region of TRPC channels results in a dominant negative function of the mutant protein (24, 25). To specifically knock down TRPC6 function, we expressed a TRPC6-YFP mutant with dominant negative character (TRPC6-DN-YFP; ref. 24) in PC12 cells. In transfected cells, selected by the YFP-fluorescence, hyperforin-induced calcium entry was dramatically reduced (see Fig. 2*D*). Our data showed that TRPC6 forms a hyperforin-responsive nonselective ion channel in PC12 cells.

# Hyperforin selectively activates HEK293 cells expressing TRPC6 channels

Based on the sequence comparison, activation mechanisms, and ability to form heteromeric channel complexes, the proteins of the TRPC group can be divided into the TRPC1, TRPC4, and TRPC5 subgroup and a subgroup activated through the diacylglycerol-activated channels TRPC3, TRPC6, and TRPC7. With respect to the controversial data of the TRPC channels endogenously expressed in PC12 cells (see Discussion), we studied HEK293 cells expressing TRPC channels (Fig. 3). In addition to the expression of TRPC proteins as C-terminal YFP fusion proteins, we controlled the functionality of the expressed proteins by the application of either OAG (100 μM) or carbachol (100 μM) prior to the application of hyperforin (10 µM). In TRPC6expressing cells, application of OAG induced a rapid increase in [Ca<sup>2+</sup>]<sub>i</sub>. The subsequent application of hyperforin resulted in a response with comparable increase in  $[Ca^{2+}]_i$  (Fig. 3A). To see whether the

activation of TRPC6 by hyperforin is specific for TRPC6 or a subgroup of TRPC channels, we next tested TRPC3 (Fig. 3*B*). To our surprise, hyperforin was ineffective to induce TRPC3-mediated calcium entry. In addition, hyperforin failed to activate TRPC4 (Fig. 3*C*). To validate these data, we additionally performed a series of experiments allowing the characterization of a large number of transfected cells. In these experiments, we exclusively applied hyperforin (Fig. 3*D*). The data showed that hyperforin selectively stimulated TRPC6.

Although our data so far provided very strong evidence for hyperforin-induced activation of TRPC6, we tested hyperforin-induced effects in electrophysiological recordings. Whole-cell recordings of TRPC6-expressing cells resulted in current-voltage relationships comparable with earlier data (Fig. 4A). In standard extracellular solutions, the current-voltage relationship of the carbachol-induced current, measured from voltage ramps, had an outwardly rectifying form, comparable with the curves resulting from hyperforin application (Fig. 4B). Maximal currents were transiently recorded 40 s after the application of hyperforin (Fig. 4C). Stable steady states were obtained 60 s after application, with mean current densities of  $-28 \pm 16$ pA/pF and  $+46 \pm 20 pA/pF$  (n=5) at -100 mV and +100 mV, respectively (Fig. 4D). In contrast, hyperforin had no effect on untransfected HEK293 cells (Fig. 4E). Enhanced inward currents and subsequent rapid desensitization were only found after application of hyperforin. Currents returned to a similar level to that before the application of hyperforin during washout phase (2 min) and removal of hyperforin.



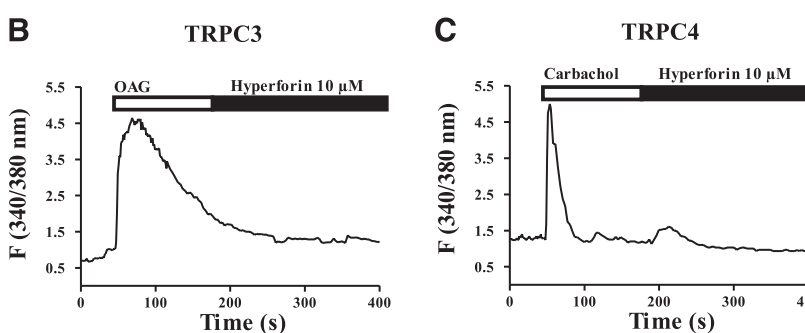


**Figure 3.** Hyperforin exclusively activates TRPC6 channels. To test whether TRPC6 or all TRPC channel proteins are activated by hyperforin, we studied effects of hyperforin in TRPC-expressing HEK293 cells in single cell measurements. TRPC proteins were transiently expressed as C-terminal YFP fusion proteins in HEK293 cells. Functional expression of the proteins was monitored by application of either OAG (100 μM) or carbachol (100 μM) before application of hyperforin (10 μM). A) Single time traces of changes in fluorescence were monitored from TRPC6-YFP-expressing HEK293 cells. Cells were consecutively stimulated with OAG (100 μM) and hyperforin (10 μM; n=6). Both substances induced changes in fluorescence indicative of enhanced intracellular calcium concentrations. B) TRPC3-YFP-expressing HEK293 cells were consecutively stimulated by OAG (100 μM) and hyperforin (10 μM; n=6). Only OAG induced

changes in fluorescence. *C*) TRPC4-YFP-expressing HEK 293 cells were consecutively stimulated with carbachol (100  $\mu$ M) and hyperforin (10  $\mu$ M; n=6). *D*) Summary of experiments of TRPC-expressing and untransfected HEK293 cells treated with hyperforin (10  $\mu$ M). Exclusively in TRPC6-expressing HEK 293 cells, hyperforin induced a significantly increased Ca<sup>2+</sup> influx. Error bars indicate sem. Data marked with asterisks are significantly different from untransfected HEK 293 cells (n=6, \*\*\*P<0.001, unpaired t test).

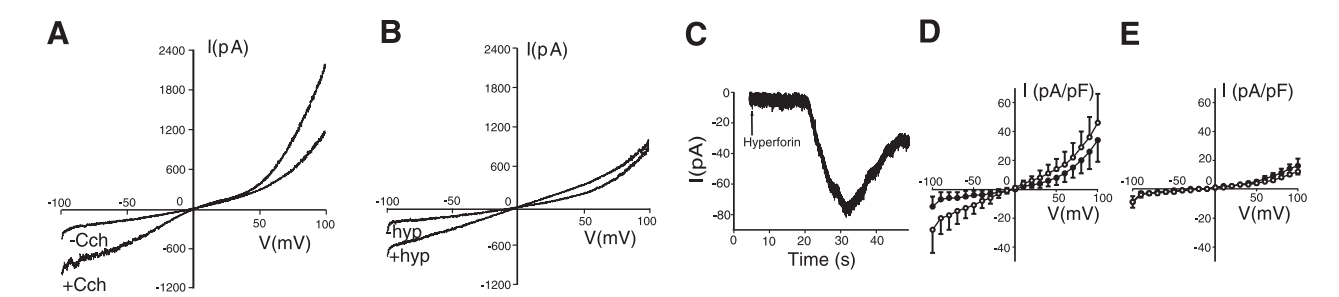


Figure 4. Hyperforin-induced, TRPC6-mediated currents. Whole-cell currents were recorded from TRPC6-expressing cells. Application of carbachol (100  $\mu$ M; *A*) and hyperforin (20  $\mu$ M; *B*) resulted in an increase in outward and inward currents. *C*) Time course of inward currents at a holding potential of -50 mV were recorded from TRPC6-expressing cells during extracellular application of hyperforin (20  $\mu$ M). Normalization of currents from TRPC6-expressing (*D*) and untransfected control cells (*E*) show that hyperforin selectively increased whole-cell currents in TRPC6-expressing cells ( $\bullet$  = before and  $\circ$  = after application of hyperforin).

For characterization of the single channel conductance, we performed inside-out recordings from TRPC6-expressing cells (n=7; **Fig. 5**). Spontaneous activity of TRPC6 was also recorded in the inside-out configuration showing a moderate open probability from the start of the recordings (see Fig. 5A). The application of hyperforin repeatedly induced an increase in channel activity within a timescale of 10 s (see Fig. 5A). Exemplary traces in the absence and presence of hyperforin are shown as insets. For further quantification of our single channel data before (Fig. 5B) and after (Fig. 5C) application of hyperforin, we calculated amplitude histograms of single-channel amplitudes. The calculation revealed that hyperforin increased the open probability of TRPC6 from 0.11 (see Fig. 5B) to 0.68 (see Fig. 5C). At the holding potential -50 mV the amplitude of the current was 1.1 pA. The chord conductance calculated from the data of our experiments is 18 pS and therefore comparable to values recently published (26).

In outside-out experiments, hyperforin-induced TRPC6 single channel activity was blocked by micromolar concentration of  $\mathrm{Gd}^{3+}$  (**Fig. 6**). Under control conditions, TRPC6 channel openings were rare (NP<sub>o</sub>=0.006±0.002, n=5) and short in duration, as also reported previously (20, 27, 28). When hyperforin was added to the bath solution at a concentration of 10  $\mu$ M, the open probability of TRPC6 was dramatically increased (NP<sub>o</sub>=0.40±0.16, n=5). Further application of  $\mathrm{Gd}^{3+}$  (100  $\mu$ M) abolished hyperforin-induced channel activity (NP<sub>o</sub>=0.0010±0.0008, n=5).

# Hyperforin induces neurite outgrowth *via* TRPC6 activation

In the brain, TRPC channels are involved in growth cone guidance and neurite extension (17–19). Therefore, we applied hyperforin to PC12, analyzed the neurite length, and compared it with NGF-treated cells.

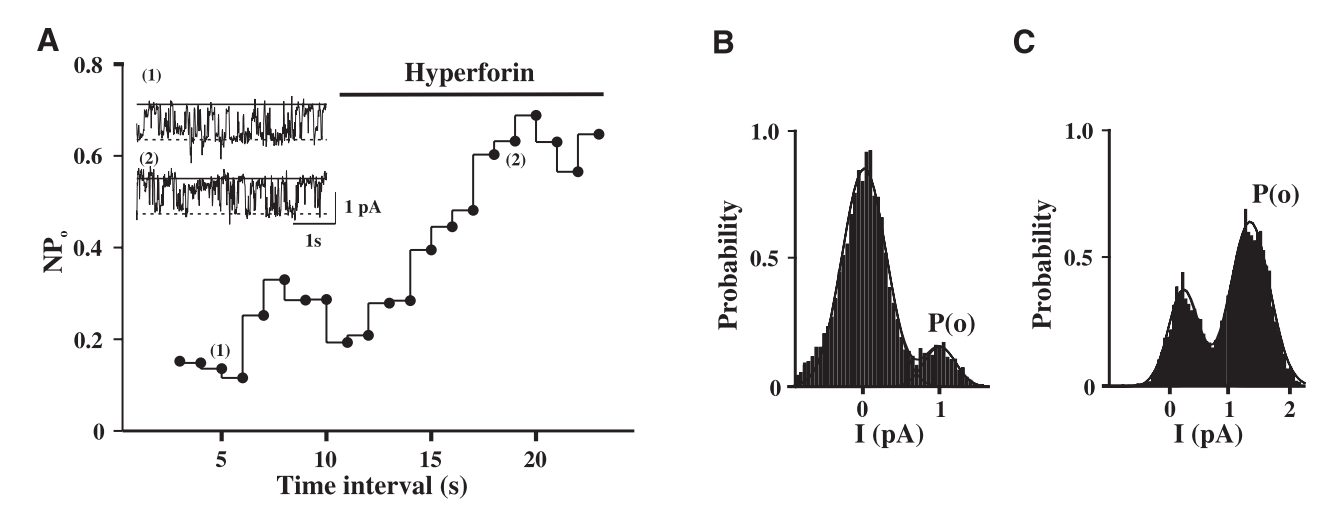
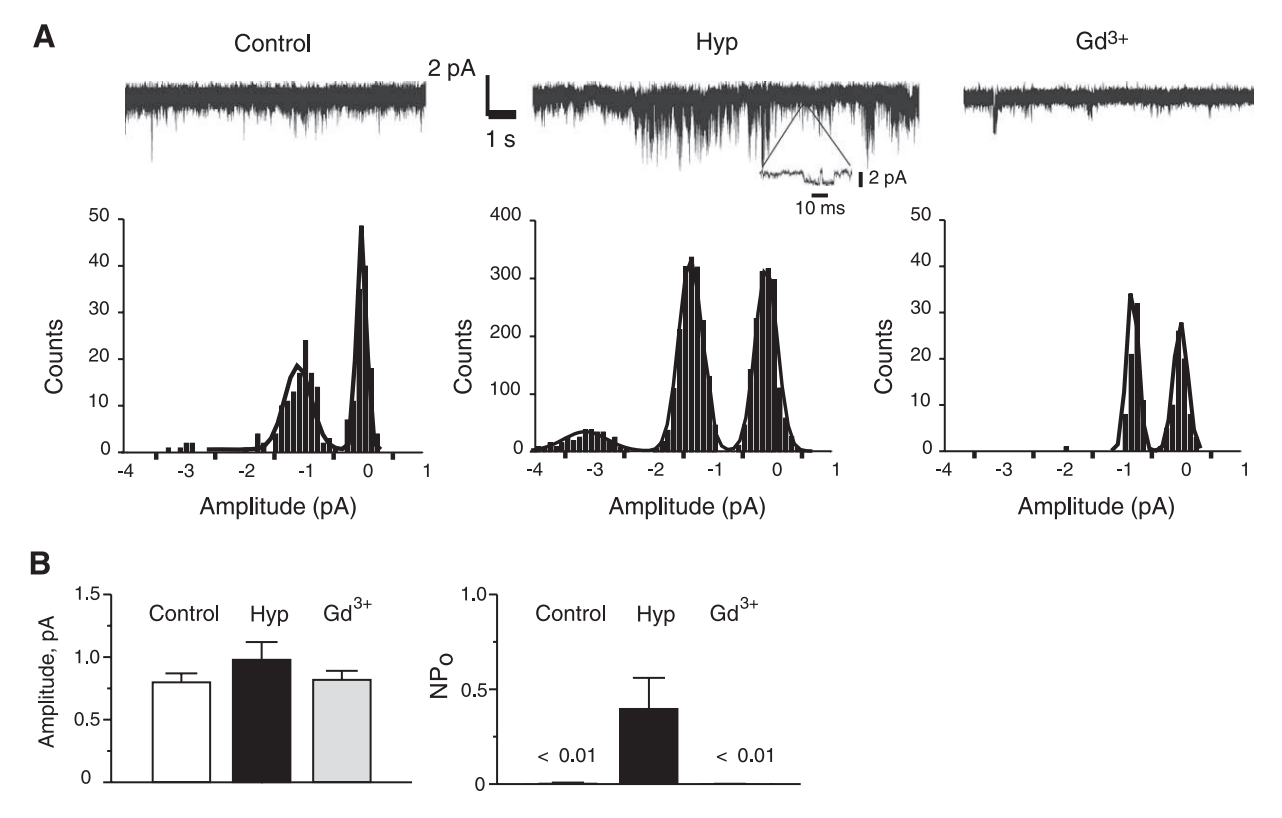


Figure 5. Single channel recordings of hyperforin-induced TRPC6. Hyperforin (20  $\mu$ M) stimulated TRPC6 channels in inside-out patches. *A)* Plot of NP<sub>o</sub> against time during a representative experiment shows the increase in channel activity after the application of the hyperforin. Insets: currents recorded at the times indicated by (1) and (2). Channel activity was recorded in inside-out patches from HEK293 cells expressing TRPC6-YFP at the holding potential of –50 mV. Statistical analysis of single-channel amplitudes were calculated from current traces of 4 s length using amplitude histograms fitted to Gaussian functions before (*B*) and after (*C*) application of hyperforin. Note change in probability of channel opening from 0.11 (*B*) to 0.68 (*C*).



**Figure 6.** Hyperforin-induced TRPC6 single channel activity is blocked by gadolinium ions. *A)* Top panels: currents recorded in outside-out patches from TRPC6-expressing cell at the holding potential of -60 mV before (left trace) and after application of  $10 \,\mu\text{M}$  hyperforin (middle trace) and  $100 \,\mu\text{M}$  Gd<sup>3+</sup> (right trace) to the bath solution. Bottom panels: amplitude distributions of detected channel openings shown on the top and calculated from current traces of  $50 \, \text{s}$  length. *B)* Left: single channel amplitudes in control (white), after application of  $10 \,\mu\text{M}$  hyperforin (black) and after  $100 \,\mu\text{M}$  Gd<sup>3+</sup> in the presence of  $10 \,\mu\text{M}$  hyperforin (gray; n=5). Right: NP<sub>o</sub> in control (white), after application of  $10 \,\mu\text{M}$  hyperforin (black), and after  $100 \,\mu\text{M}$  Gd<sup>3+</sup> (gray) (n=5).

To test clinically relevant concentrations, we applied hyperforin in concentrations that are reached in plasma of patients and in brain homogenates of mice after treatment with clinical relevant doses of St. John's wort extract or hyperforin (29, 30). Hyperforin in the clinically relevant concentrations of 0.1 and 0.3 μM induce modest Ca<sup>2+</sup>- and Na<sup>+</sup>-influx (9). In side-by-side experiments, PC12 cells were incubated for 5 days with either hyperforin or NGF (50 ng/ml; **Fig. 7**). Differentiation of PC12 cells was analyzed by measuring the neurite length of PC12 cells after 5 days (Fig. 7*A*, *B*). Hyperforin had similar effects on PC12 cell differentiation as NGF; both induced a significant neurite outgrowth (see Fig. 7*A*, *B*).

To determine whether TRPC6 channel activation is involved in hyperforin-mediated differentiation of PC12 cells, we coincubated hyperforin (0.3  $\mu$ M) with La³+ (100  $\mu$ M) and Gd³+ (100  $\mu$ M) as channel blockers for 5 days. Under these conditions hyperforininduced differentiation and neurite outgrowth was abolished (Fig. 7*C*). To further test the role of TRPC6 channels for hyperforin-mediated differentiation, PC12 cells were transiently transfected with anti-TRPC6 RNAi 2 and with the plasmid coding for the dominant negative TRPC6 mutant and subsequently treated with hyperforin (0.3  $\mu$ M) for 3 days. In cells transfected with anti-TRPC6 RNAi 2, hyperforin-induced neurite out-

growth was strongly diminished compared to cells treated with control RNAi of low GC content (Fig. 7*D*). In addition, cells expressing the TRPC6-DN-YFP showed a strongly reduced neurite outgrowth (Fig. 7*E*). The results of both independent approaches knocking down TRPC6 function in PC12 cells strongly argue for the involvement of TRPC6 in the hyperforin-induced differentiation of PC12 cells.

### **DISCUSSION**

An approach combining pharmacological profiling and molecular biological RT-PCR analysis allowed us to unravel the molecular target of hyperforin in the central nervous system. Our data show that hyperforin activates TRPC6, resulting in immediately increased intracellular sodium and calcium concentrations and induction of neurite outgrowth.

As a model system for our analysis of hyperforininduced effects, we used PC12 cells, a rat pheochromocytoma cell line, commonly used in studies analyzing neuronal signaling cascades and screening compounds for neurotrophic properties. With respect to the pattern of TRPC channels expressed in this cell line, we found quite different data in the literature. Based on RT-PCR analysis, a variety of TRPC channel combina-

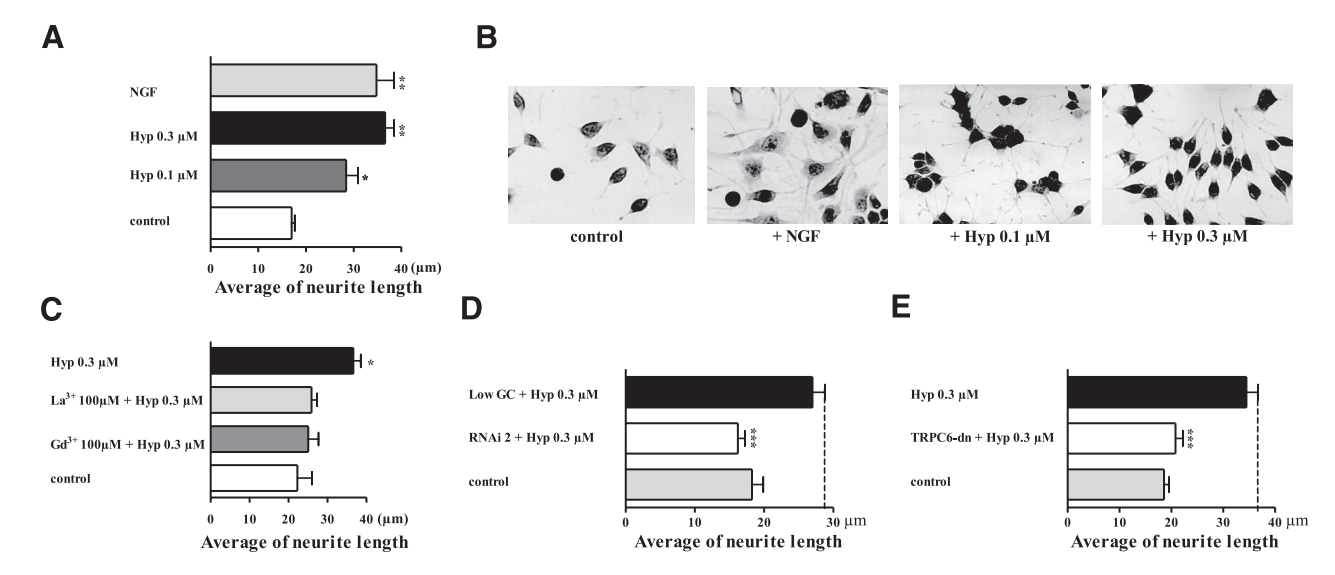


Figure 7. Hyperforin-induced neurite outgrowth in PC12 cells. *A*) PC12 cells were treated with hyperforin (0.1 and 0.3 μM) or NGF (50 ng/ml). After a 3 day incubation period the average neurite extension was measured and the data of hyperforin-treated cells were compared to NGF-stimulated PC12 cells. *B*) Representative images of PC12 cells showing neurite extensions are shown from experiments after a 5 day incubation period in the presence of hyperforin (0.1 and 0.3) or NGF (50 ng/ml; n=6). *C*) Average neurite extension induced by hyperforin was compared to PC12 cells additionally treated with La<sup>3+</sup> (100 μM) or Gd<sup>3+</sup> (100 μM) for 5 days. For *A* and *C*, error bars indicate sem. Data marked with asterisks are significantly different from controls (n=6, \*P<0.05, \*\*P<0.01 unpaired t test). *D*) siRNA electroporated cells with RNAi 2 and electroporated cells with low GC control were treated with hyperforin (0.3 μM) 24 h after electroporation. After 3 days representative images were taken and neuritic outgrowth was measured. Data given in bars compare hyperforin-induced neurite outgrowth in RNAi 2-electroporated with asterisks are significantly different from controls (n=3, \*\*\*P<0.001, unpaired t test). *E*) TRPC6-DN-YFP-expressing and untransfected PC12 cells were treated with hyperforin (0.3 μM) 24 h after transfection and differentiated over 3 consecutive days. Representative images were taken and neurite lengths were measured. The data given in the bars compare hyperforin-induced neurite outgrowth in TRPC6-DN-YFP-expressing and untransfected PC12 cells. Error bars indicate sem. Data marked with asterisks are significantly different from controls (n=6, \*\*\*P<0.001, unpaired t test).

tions have been identified in PC12 cells (31–34). The number of identified TRPC channels ranged from two TRPC channels to nearly all members of the TRPC channel family. The latter was quite surprising, as many propose, for example, that TRPC3, TRPC6, and TRPC7 are functionally redundant proteins. Independently from TRPC channels identified by RT-PCR, there is strong evidence for the exclusive functional expression of TRPC6 in PC12 cells. In nearly all publications studying functions of endogenously expressed channels, the effects have been assigned to TRPC6 expression (31, 32, 34). Only one recent publication on the indirect regulation of TRPC3 by the TFII-transcription factors assigned the effect to TRPC3 (35). Nevertheless, it was necessary to analyze the TRPC channel protein expressed in PC12 cells having been used in our experiments. Therefore, we performed Western blot analyses. As already shown by Tesfai et al. (31), the Western blot analyses revealed that TRPC6 was expressed in PC12 cells. The detection was suppressed in the presence of the peptide used for immunization, indicating that the antibody specifically detected the TRPC6 protein. Furthermore, in PC12 cells electroporated with siRNA directed against TRPC6, the signals of the detection reaction were dramatically reduced, providing additional evidence for the specificity of the

detection reaction performed in the presence of the anti-TRPC6 antibody.

Corresponding to the structures of other cation channel families, it is accepted that the pores formed by TRP channels are composed of four channel proteins. Experimental evidence results from various studies showing that TRP channels form homomeric as well as in a limited amount heteromeric channel complexes (24, 36, 37). For the members of the TRPC subfamily, it has been shown by cotrafficking-, FRET-, and coimmunoprecipitation analyses that TRPC channels exclusively assemble into homomeric channel complexes and into heteromeric channel complexes within the narrow confines of phylogenetically closely related channels, *i.e.*, the TRPC4/TRPC5 and TRPC3/TRPC6/TRPC7 subgroups (24).

The specific assembly of TRPC channels into multimeric pore-forming protein complexes is the basis for an elegant inactivation approach. In contrast to antisense or siRNA approaches targeting the mRNAs coding for TRPC channels, the approach of expression of TRPC mutants with dominant negative character allows the inactivation of TRPC channel function independent from stability of mRNA species and the half lives of the TRPC proteins in the given endogenous context. The use of expression constructs using fluorescence

protein tags further improves this method, allowing control of the expression of the protein simultaneously with functional analyses. TRPC mutants with dominant negative character have already been described (24, 37). We used a corresponding TRPC6 mutant in our functional studies. Both biological effects, hyperforin-induced calcium entry and hyperforin-induced neurite outgrowth, were dramatically reduced in cells expressing the mutant, arguing for the involvement of TRPC6 channels in the hyperforin-induced biological effect in PC12 cells.

On the other hand, the potency of forming heteromeric channel complexes within the TRPC3, TRPC6, and TRPC7 subgroup made it necessary to test whether TRPC6 or all members of the TRPC family are activated by hyperforin. The data were very impressive, showing a highly selective activation solely of TRPC6 by hyperforin. This means that hyperforin is the first selective activator of a TRPC channel protein. We characterized this unique activation mechanism using electrophysiological recordings showing that the hyperforin activation results in currents comparable to currents induced by carbachol or diacylglycerol. The activation of TRPC6 in the excised patch configuration furthermore argues for a direct interaction of hyperforin with the channel protein.

TRPC channels play an important role for growth cone guidance and neurite extension in the brain (17–19). Soon after the first characterization of TRPC channels as receptor-stimulated cation channels regulated in a phospholipase C-dependent manner, the participation of TRPC3 in BDNF-triggered signaling was demonstrated (38). In the meantime, it has additionally been shown that TRPC1 is involved in netrin-1 and BDNF-induced axon turning in Xenopus neurons (18), whereas TRPC5 is enriched in growth cones of cultured mouse hippocampal neurons and negatively regulates neurite extension in these cells. Contrary to these findings, a recent study reported that BDNFinduced cone attraction in cultured rat cerebral granule cells is mediated by Ca<sup>2+</sup> elevation through activation of TRPC3 and TRPC6 (17). A recent proteomic analysis of interacting proteins supports the view that TRPC6 is involved in postsynaptic signaling and synaptic plasticity (19).

In summary, our data deorphanize the molecular target of hyperforin in brain by demonstrating that hyperforin activates TRPC6-mediated currents changing intracellular sodium and calcium concentrations. Hyperforin-induced, TRPC6-mediated sodium currents elevating the intracellular sodium concentration may indirectly reduce monoamine uptake by decreasing the sodium gradient as the driving force of the neurotransmitter transporters. On the other hand, the hyperforin-induced, TRPC6-mediated calcium entry mimics neurotrophic effect of NGF or BDNF. The combination of both biological effects, which are of particular relevance for antidepressant drug response (39), provides a molecular rationale for the pharmacological profile of hyperforin.

We thank Inge Reinsch for technical assistance, Michael Schaefer for providing the TRPC cDNAs and Ruth and Sebastian Schaffer for language editing. The authors are supported by the Deutsche Forschungsgemeinschaft, Dr. Willmar Schwabe, and Sonnenfeld-Stiftung.

#### REFERENCES

- Müller, W. E. (2003) Current St John's wort research from mode of action to clinical efficacy. *Pharmacol. Res.* 47, 101–109
- 2. Williams, J. W., and Jr., Holsinger, T. (2005) St John's for depression, worts and all. *BMJ* 330, E350–E351
- 3. Szegedi, A., Kohnen, R., Dienel, A., and Kieser, M. (2005) Acute treatment of moderate to severe depression with hypericum extract WS 5570 (St John's wort): randomised controlled double blind non-inferiority trial versus paroxetine. *BMJ* 330, 503
- Lecrubier, Y., Clerc, G., Didi, R., and Kieser, M. (2002) Efficacy of St. John's wort extract WS 5570 in major depression: a double-blind, placebo-controlled trial. *Am.J. Psychiatry.* 159, 1361–1366
- Kasper, S., Anghelescu, I. G., Szegedi, A., Dienel, A., and Kieser, M. (2006) Superior efficacy of St John's wort extract WS 5570 compared to placebo in patients with major depression: a randomized, double-blind, placebo-controlled, multi-center trial. BMC Med. 4, 14
- Linde, K., Mulrow, C. D., Berner, M., and Egger, M. (2005) St John's wort for depression. *Cochrane. Database. Syst. Rev.* CD000448
- Wonnemann, M., Singer, A., and Müller, W. E. (2000) Inhibition of synaptosomal uptake of 3H-L-glutamate and 3H-GABA by hyperforin, a major constituent of St. John's Wort: the role of amiloride sensitive sodium conductive pathways. *Neuropsycho-pharmacology* 23, 188–197
- Singer, A., Wonnemann, M., and Müller, W. E. (1999) Hyperforin, a major antidepressant constituent of St. John's wort, inhibits serotonin uptake by elevating free intracellular Na<sup>+</sup>.
   J. Pharmacol. Exp. Ther. 290, 1363–1368

   Treiber, K., Singer, A., Henke, B., and Müller, W. E. (2005)
- Treiber, K., Singer, A., Henke, B., and Müller, W. E. (2005) Hyperforin activates nonselective cation channels (NSCCs). Br. J. Pharmacol. 145, 75–83
- Montell, C., Birnbaumer, L., and Flockerzi, V. (2002) The TRP channels, a remarkably functional family. *Cell* 108, 595–598
- Clapham, D. E. (2003) TRP channels as cellular sensors. *Nature* 426, 517–524
- Harteneck, C. (2005) Function and pharmacology of TRPM cation channels. Naunyn-Schmiedebergs. Arch. of. Pharmacol. 371, 307–314
- Harteneck, C., Grimm, C., Kraft, R., and Schultz, G. (2005) Activation of TRPM3 by sphingosine. *Naunyn-Schmiedebergs Arch. Pharmacol.* 371, R54
- Kraft, R., and Harteneck, C. (2005) The mammalian melastatinrelated transient receptor potential cation channels: an overview. *Plügers Arch.* 451, 204–211
- Riccio, A., Medhurst, A. D., Mattei, C., Kelsell, R. E., Calver, A. R., Randall, A. D., Benham, C. D., and Pangalos, M. N. (2002) mRNA distribution analysis of human TRPC family in CNS and peripheral tissues. *Mol. Brain. Res.* 109, 95–104
- Kunert-Keil, C., Bisping, F., Kruger, and J., Brinkmeier, H. (2006) Tissue-specific expression of TRP channel genes in the mouse and its variation in three different mouse strains. BMC Genomics. 7, 159
- Li, Y., Jia, Y. C., Cui, K., Li, N., Zheng, Z. Y., Wang, Y. Z., and Yuan, X. B. (2005) Essential role of TRPC channels in the guidance of nerve growth cones by brain-derived neurotrophic factor. *Nature* 434, 894–898
- Wang, G. X., and Poo, M. M. (2005) Requirement of TRPC channels in netrin-1-induced chemotropic turning of nerve growth cones. *Nature* 434, 898–904
- Greka, A., Navarro, B., Oancea, E., Duggan, A., and Clapham,
   D. E. (2003) TRPC5 is a regulator of hippocampal neurite length and growth cone morphology. *Nat. Neurosci.* 6, 837–845
- 20. Hofmann, T., Obukhov, A. G., Schaefer, M., Harteneck, C., Gudermann, T., and Schultz, G. (1999) Direct activation of

- human TRPC6 and TRPC3 channels by diacylglycerol. *Nature* **397**, 259–263
- Grimm, C., Kraft, R., Sauerbruch, S., Schultz, G., and Harteneck, C. (2003) Molecular and functional characterization of the melastatin-related cation channel TRPM3. J. Biol. Chem. 278, 21493–21501
- 22. Kwan, C. Y., and Putney, J. W., Jr. (1990) Uptake and intracellular sequestration of divalent cations in resting and methacholine-stimulated mouse lacrimal acinar cells. Dissociation by Sr<sup>2+</sup> and Ba<sup>2+</sup> of agonist-stimulated divalent cation entry from the refilling of the agonist-sensitive intracellular pool. *J. Biol. Chem.* 265, 678–684
- Vazquez, G., Wedel, B. J., Aziz, O., Trebak, M., and Putney, J. W., Jr. (2004) The mammalian TRPC cation channels. *Biochim. Biophys. Acta* 1742, 21–36
- Hofmann, T., Schaefer, M., Schultz, G., and Gudermann, T. (2002) Subunit composition of mammalian transient receptor potential channels in living cells. *Proc. Natl. Acad. Sci. U. S. A.* 99, 7461–7466
- Hellwig, N., Albrecht, N., Harteneck, C., Schultz, G., and Schaefer, M. (2005) Homo- and heteromeric assembly of TRPV channel subunits. J. Cell Sci. 118, 917–928
- Large, W. A. (2002) Receptor-operated Ca2(+)-permeable nonselective cation channels in vascular smooth muscle: a physiologic perspective. *J. Cardiovasc. Electrophysiol.* 13, 493–501
- Hisatsune, C., Kuroda, Y., Nakamura, K., Inoue, T., Nakamura, T., Michikawa, T., Mizutani, A., and Mikoshiba, K. (2004) Regulation of TRPC6 channel activity by tyrosine phosphorylation. *J. Biol. Chem.* 279, 18887–18894
- Jung, S., Mühle, A., Schaefer, M., Strotmann, R., Schultz, G., and Plant, T. D. (2003) Lanthanides potentiate TRPC5 currents by an action at extracellular sites close to the pore mouth. *J. Biol. Chem.* 278, 3562–3571
- Biber, A., Fischer, H., Römer, A., and Chatterjee, S. S. (1998)
   Oral bioavailability of hyperforin from hypericum extracts in rats and human volunteers. *Pharmacopsychiatry* 31, Suppl. 1, 36–43
- 30. Keller, J. H., Karas, M., Müller, W. E., Volmer, D. A., Eckert, G. P., Tawab, M. A., Blume, H. H., Dingermann, T., and

- Schubert-Zsilavecz, M. (2003) Determination of hyperforin in mouse brain by high-performance liquid chromatography/tandem mass spectrometry. *Anal. Chem.* **75**, 6084–6088
- Tesfai, Y., Brereton, H. M., and Barritt, G. J. (2001) A diacylglycerol-activated Ca<sup>2+</sup> channel in PC12 cells (an adrenal chromaffin cell line) correlates with expression of the TRP-6 (transient receptor potential) protein. *Biochem. J.* 358, 717–726
- 32. Mwanjewe, J., and Grover, A. K. (2004) Role of transient receptor potential canonical 6 (TRPC6) in non-transferrinbound iron uptake in neuronal phenotype PC12 cells. *Biochem. J.* **378**, 975–982
- 33. Ohta, T., Morishita, M., Mori, Y., and Ito, S. (2004) Ca<sup>2+</sup> store-independent augmentation of [Ca<sup>2+</sup>]<sub>(i)</sub> responses to G-protein coupled receptor activation in recombinantly TRPC5-expressed rat pheochromocytoma (PC12) cells. *Neuroscience Letters* **358**, 161–164
- Kim, J. Y., Saffen, D. (2005) Activation of M1 muscarinic acetylcholine receptors stimulates the formation of a multiprotein complex centered on TRPC6 channels. *J. Biol. Chem.* 280, 32035–32047
- Caraveo, G., van Rossum, D. B., Patterson, R. L., Snyder, S. H., and Desiderio, S. (2006) Action of TFII-I outside the nucleus as an inhibitor of agonist-induced calcium entry. Science 314, 122–125
- Strubing, C., Krapivinsky, G., Krapivinsky, L., and Clapham, D. E. (2003) Formation of novel TRPC channels by complex subunit interactions in embryonic brain. *J. Biol. Chem.* 278, 39014–39019
- Strubing, C., Krapivinsky, G., Krapivinsky, L., and Clapham, D. E. (2001) TRPC1 and TRPC5 form a novel cation channel in mammalian brain. *Neuron* 29, 645–655
- Li, H. S., Xu, X. Z., and Montell, C. (1999) Activation of a TRPC3-dependent cation current through the neurotrophin BDNF. Neuron. 24, 261–273
- Duman, R. S. (2004) Depression: A case of neuronal life and death? *Biol. Psychiatry.* 56, 140–145

Received for publication February 5, 2007. Accepted for publication June 27, 2007.